

AD

TECHNICAL REPORT ARCCB-TR-97004

**STRESS CONCENTRATION, STRESS INTENSITY, AND FATIGUE  
LIFETIME CALCULATIONS IN AUTOFRETTAGED TUBES  
CONTAINING AXIAL PERFORATIONS WITHIN THE WALL**

**ANTHONY P. PARKER  
STEPHEN N. ENDERSBY  
TIMOTHY J. BOND**

**JOHN H. UNDERWOOD  
SABRINA L. LEE  
JOHN HIGGINS**

FEBRUARY 1997

	<p><b>US ARMY ARMAMENT RESEARCH, DEVELOPMENT AND ENGINEERING CENTER CLOSE COMBAT ARMAMENTS CENTER BENÉT LABORATORIES WATERVLIET, N.Y. 12189-4050</b></p>	
---	--	---

APPROVED FOR PUBLIC RELEASE; DISTRIBUTION UNLIMITED

DTIC QUALITY INSPECTED 3

19970414 051

### DISCLAIMER

The findings in this report are not to be construed as an official Department of the Army position unless so designated by other authorized documents.

The use of trade name(s) and/or manufacturer(s) does not constitute an official indorsement or approval.

### DESTRUCTION NOTICE

For classified documents, follow the procedures in DoD 5200.22-M, Industrial Security Manual, Section II-19 or DoD 5200.1-R, Information Security Program Regulation, Chapter IX.

For unclassified, limited documents, destroy by any method that will prevent disclosure of contents or reconstruction of the document.

For unclassified, unlimited documents, destroy when the report is no longer needed. Do not return it to the originator.

# REPORT DOCUMENTATION PAGE

Form Approved  
OMB No. 0704-0188

Public reporting burden for this collection of information is estimated to average 1 hour per response, including the time for reviewing instructions, searching existing data sources, gathering and maintaining the data needed, and completing and reviewing the collection of information. Send comments regarding this burden estimate or any other aspect of this collection of information, including suggestions for reducing this burden, to Washington Headquarters Services, Directorate for Information Operations and Reports, 1215 Jefferson Davis Highway, Suite 1204, Arlington, VA 22202-4302, and to the Office of Management and Budget, Paperwork Reduction Project (0704-0188), Washington, DC 20503.

<b>1. AGENCY USE ONLY (Leave blank)</b>	<b>2. REPORT DATE</b> February 1997	<b>3. REPORT TYPE AND DATES COVERED</b> Final	
<b>4. TITLE AND SUBTITLE</b> STRESS CONCENTRATION, STRESS INTENSITY, AND FATIGUE LIFETIME CALCULATIONS IN AUTOFRETTAGED TUBES CONTAINING AXIAL PERFORATIONS WITHIN THE WALL		<b>5. FUNDING NUMBERS</b> AMCMS No. 6226.24.H180.0 PRON No. TU5A5F361ABJ	
<b>6. AUTHOR(S)</b> Anthony P. Parker (Royal Military College of Science, Cranfield Univ., UK), Stephen N. Endersby (U. of Northumbria, UK), Timothy J. Bond (U. of Northumbria, UK), John H. Underwood, Sabrina L. Lee, and John Higgins			
<b>7. PERFORMING ORGANIZATION NAME(S) AND ADDRESS(ES)</b> U.S. Army ARDEC Benet Laboratories, AMSTA-AR-CCB-O Watervliet, NY 12189-4050		<b>8. PERFORMING ORGANIZATION REPORT NUMBER</b> ARCCB-TR-97004	
<b>9. SPONSORING / MONITORING AGENCY NAME(S) AND ADDRESS(ES)</b> U.S. Army ARDEC Close Combat Armaments Center Picatinny Arsenal, NJ 07806-5000		<b>10. SPONSORING / MONITORING AGENCY REPORT NUMBER</b>	
<b>11. SUPPLEMENTARY NOTES</b> Presented at the ASME Pressure Vessels and Piping Conference, Montreal, Canada, 22-26 July 1996. Published in proceedings of the conference.			
<b>12a. DISTRIBUTION / AVAILABILITY STATEMENT</b> Approved for public release; distribution unlimited.		<b>12b. DISTRIBUTION CODE</b>	
<b>13. ABSTRACT (Maximum 200 words)</b>  Elastic, elastic-plastic, and experimental stress analyses and fatigue lifetime predictions are presented for thick cylinders containing multiple, axial holes within the wall. The holes are generally semi-elliptical (including semi-circular) and the cylinders are autofrettaged after introduction of the holes and are subsequently subjected to cyclic pressurization of the bore.  Two potentially critical failure locations are identified; a fracture-mechanics based design methodology is proposed; elastic and elastic-plastic finite element (FE) analyses are undertaken. The elastic FE analysis predicts hoop stresses at the bore resulting from internal pressurization which are some 7% higher than those for the equivalent plain tube. For a given hole size and location and for nominal overstrains of 40% or greater, the residual compressive stress at the bore is reduced by approximately 15% below the value for a plain tube of the same radius ratio.  Two experimental investigations are reported, one based upon X-ray diffraction, to measure residual stresses, and the other based upon radial tube slitting, to measure opening angle. They confirm most features of the residual stress profiles predicted from FE analysis, with the exception of high compressive residual stresses and stress gradients immediately adjacent to the hole boundaries. Appropriate use of the residual stress information permits prediction of tube lifetimes for cracks emanating from the bore and from the hole. For the geometry and loading under consideration, the more critical location is predicted to be the hole boundary, the lifetime for failures originating from this point being some 60% of the lifetime for cracks originating at the bore.			
<b>14. SUBJECT TERMS</b> Autofrettage, Crack Growth, Fatigue Cracks, Cylinders, Channels, Fracture (Materials), Fracture Mechanics, Residual Stress, Stress Concentration Factor, Stress Intensity Factor		<b>15. NUMBER OF PAGES</b> 15	
<b>17. SECURITY CLASSIFICATION OF REPORT</b> UNCLASSIFIED		<b>16. PRICE CODE</b>	
<b>18. SECURITY CLASSIFICATION OF THIS PAGE</b> UNCLASSIFIED	<b>19. SECURITY CLASSIFICATION OF ABSTRACT</b> UNCLASSIFIED	<b>20. LIMITATION OF ABSTRACT</b> UL	

## TABLE OF CONTENTS

	<u>Page</u>
INTRODUCTION .....	1
A POSSIBLE DESIGN METHODOLOGY .....	2
ELASTIC FINITE ELEMENT ANALYSIS .....	2
Commentary .....	3
ELASTIC-PLASTIC FINITE ELEMENT ANALYSIS .....	3
Commentary .....	3
X-RAY MEASUREMENTS OF RESIDUAL STRESS .....	4
RING SLICING ANALYSIS OF RESIDUAL STRESS .....	4
Recommendations .....	4
IMPLICATIONS FOR FATIGUE LIFETIME .....	4
Commentary .....	5
SUMMARY AND CONCLUSIONS .....	5
ACKNOWLEDGEMENTS .....	5
REFERENCES .....	6

### TABLES

1. Effect of Hole Eccentricity on Stress Concentration Factor .....	7
2. Reduced Bore Compressive Hoop Stress .....	7
3. Lifetimes for Pre-Cracked Tubes with Semi-Circular Holes, Failure Originating from Bore .....	7

### LIST OF ILLUSTRATIONS

1. Schematic Illustration of Geometry Considered .....	8
2. Specific Hole Geometries Analysed Using Finite Element Methods .....	8
3. Typical Finite Element Mesh Used in Stress Analysis .....	9
4. Relationship Between Eccentricity of Semi-Ellipse and Stress Concentration Factor .....	9

5.	Hoop Stresses in Perforated Tube, Bore to Hole .....	10
6.	Contours of Plastic Strain at Peak of Autofrettage Cycle .....	10
7.	60% Nominal Swage Autofrettage Stresses - Semi-Circular and Offset Semi-Elliptical Holes .....	11
8.	Swage Autofrettage with Semi-Circular Holes - 20%, 40%, 60%, 80% Nominal Overstrain .....	12
9.	X-Ray Diffraction Residual Stress Measurements Compared to Proposed Bound .....	13
10.	Form of Remaining, Inner Externally Notched Tube Which was Subsequently Opened by Radial Slitting .....	13

# STRESS CONCENTRATION, STRESS INTENSITY AND FATIGUE LIFETIME CALCULATIONS IN AUTOFRETTAGED TUBES CONTAINING AXIAL PERFORATIONS WITHIN THE WALL

Anthony P Parker

Royal Military College of Science  
Cranfield University  
SWINDON, SN6 8LA, UK

Stephen N Endersby<sup>1</sup>

Timothy J Bond<sup>1</sup>

<sup>1</sup>University of Northumbria  
NEWCASTLE UPON TYNE, NE1 8ST, UK

John H Underwood<sup>2</sup>

Sabrina L Lee<sup>2</sup>

John Higgins<sup>2</sup>

<sup>2</sup>Army Armament R D & E Center  
Watervliet, NY 12189

## ABSTRACT

Elastic, elastic-plastic and experimental stress analyses and fatigue lifetime predictions are presented for thick cylinders containing multiple, axial holes within the wall. The holes are generally semi-elliptical (including semi-circular) and the cylinders are autofrettaged after introduction of the holes and are subsequently subjected to cyclic pressurization of the bore.

Two potentially critical failure locations are identified: a fracture-mechanics based design methodology is proposed: elastic and elastic-plastic finite element (FE) analyses are undertaken. The elastic FE analysis predicts hoop stresses at the bore resulting from internal pressurization which are some 7% higher than those for the equivalent plain tube. For a given hole size and location and for nominal overstrains of 40% or greater the residual compressive stress at the bore is reduced by approximately 15% below the value for a plain tube of the same radius ratio.

Two experimental investigations are reported, one based upon X-ray diffraction, to measure residual stresses, and the other based upon radial tube slitting, to measure opening angle. They confirm most features of the residual stress profiles predicted from FE analysis with the exception of high compressive residual stresses and stress gradients immediately adjacent to the hole boundaries. Appropriate use of the residual stress information permits prediction of tube lifetimes for cracks emanating from the bore and from the hole. For the geometry and loading under consideration the more critical location is predicted to be the hole boundary, the lifetime for failures originating from this point being some 60% of the lifetime for cracks originating at the bore.

## KEY WORDS

autofrettage, crack growth, fatigue cracks, cylinders, channels, fracture (materials), fracture mechanics, residual stress, stress concentration factor, stress intensity factor

## INTRODUCTION

The use of autofrettage to enhance fatigue lifetimes of thick cylinders subjected to internal cyclic pressurization is well known and relatively well understood. Recent work has addressed the problems associated with geometrical changes which remove the initial axi-symmetric nature of geometry and stressing of these tubes, namely:

- a. Axial erosion grooves, which arise after autofrettage, along the bore of the cylinder, [1].
- b. Cross-bore holes normal to the tube axis [2] and inclined at an angle to the axis [3]. These holes likewise are introduced after autofrettage.

The purpose of the work presented herein is to analyze, using elastic and elastic/plastic stress analysis methods and experimental measurements of residual stress, the fatigue behaviour of cylinders which contain a series of equally spaced holes orientated parallel to the tube axis and which were introduced prior to autofrettage. The cross-sectional shape of these holes may be somewhat arbitrary, but is shown diagrammatically in Figure 1 as circular.

The overall program of work was phased to permit development of simple models which might provide a design

methodology and would also provide a basis for checking and verifying results obtained from more sophisticated elastic and elastic/plastic numerical analyses and experimental residual stress measurements.

### A POSSIBLE DESIGN METHODOLOGY

Experience indicates that two potentially critical failure locations are on a radial line at the point on the hole closest to the bore and on the bore itself. Assume pre-existing crack-like defects at the bore and hole of depth  $a_B$  and  $a_H$  respectively and positive cyclic hoop stresses of  $\Delta(\sigma_B + p)$  and  $\Delta\sigma_H$  respectively where  $\sigma_B$  and  $\sigma_H$  represent the positive part of the cyclic hoop stress loading at the bore and hole arising from cyclic pressurization of the bore and  $p$  accounts for pressure infiltrating the bore crack. The stress intensity factor ranges at hole and bore are given, respectively by:

$$\Delta K_H = 1.12\Delta(\sigma_H) \cdot \sqrt{\pi a_H} \quad (1)$$

$$\Delta K_B = 1.12\Delta(\sigma_B + p) \cdot \sqrt{\pi a_B} \quad (2)$$

Now define a stress range ratio,  $R\Delta$  as:

$$R\Delta = \frac{\Delta\sigma_H}{\Delta(\sigma_B + p)} \quad (3)$$

The expression for lifetime at any two potential fatigue failure locations is developed in [4]. The ratio of lives for failure solely from Location 1 ( $N_1$ ) and failure solely from Location 2 ( $N_2$ ) is:

$$\frac{N_2}{N_1} = \left[ \frac{\Delta\sigma_1}{\Delta\sigma_2} \right]^m \cdot \left[ \frac{a_2}{a_1} \right]^{1-m/2} \quad (4)$$

where  $m$  is the Paris' law exponent, often approximately 3, and  $\Delta\sigma_1$ ,  $\Delta\sigma_2$ ,  $a_1$ ,  $a_2$  are stress ranges and initial crack lengths at Locations 1 and 2 respectively.

For the case of interest here, identifying Location 1 with the bore and Location 2 with the hole, the above equation becomes:

$$\frac{N_H}{N_B} = \left[ \frac{1}{R\Delta} \right]^m \cdot \left[ \frac{a_H}{a_B} \right]^{1-m/2} \quad (5)$$

Equation 5 will be employed later in the prediction of lifetimes and initial defect ratios from existing data.

Since, for equal lifetimes at both locations, the ratio  $N_H/N_B$  in equation 5 will be unity:

$$R\Delta_{\text{Equal_Lifetimes}} = \left[ \frac{a_H}{a_B} \right]^{(1/m-1/2)} \quad (6)$$

It is important to interpret this result correctly. It means that to protect against failure originating from the hole as a critical location the stress range ratio,  $R\Delta$ , should not exceed the calculated value. It is therefore a maximum design value and not a target.

### ELASTIC FINITE ELEMENT ANALYSIS

Several possible designs were analyzed using an elastic Finite Element program (RASNA). In all cases they consist of a cyclic array of 24 equally-spaced holes. The holes are of two possible designs, semi-elliptical (including semi-circular, this being Case 1) and offset semi-elliptical (this being Case 2) illustrated in Figure 2.

A typical FE mesh for these configurations is shown in Figure 3. Taking full advantage of symmetries it is only necessary to model some 360/(24x2) or 7.5 degrees of the tube. A pressure of 406 MPa was applied to the bore whilst essential symmetry conditions were ensured by imposing  $u_\theta = 0$ ,  $\tau_{r\theta} = 0$  on all radii of symmetry, where  $u_\theta$  represents displacement normal to a line of radial symmetry and  $\tau_{r\theta}$  is the shear stress along this line.

Table 1 gives stress concentration data. The maximum hoop stress occurs on the hole boundary at the point closest to the bore. The stress concentration factors,  $K_t$  at this location (based on hoop stress at the critical location in the absence of the channel, i.e. Lamé's hoop stress) for Case 1 and Case 2 are 2.64 and 2.07 respectively. These may be compared with the simple approach developed in [5] and based upon an elastic biaxial stress field model which takes account of multiple holes and employs stress concentration data from [6, 7 and 8] which predicted 2.61 and 2.07 respectively. Agreement is considered good.

An extended parameter study was also undertaken using FE. This involved varying the ellipse eccentricity and also determining  $K_t$  at locations A and B, Figure 4. These results are presented graphically in Figure 4 and numerically in Table 1 and indicate that the critical location on the hole boundary will always be the point nearest the bore. Nevertheless relatively high stresses can occur at point B, radially opposite the critical location on the outer tube. Point C (the sharp corner) is liable to produce a localized stress singularity. The significance of this point is discussed later in relation to plasticity effects.

A plot of the hoop stress variation on a radial line from bore to hole is presented for Cases 1 and 2 (Figure 5). This includes the upper SCF limits of 2.61 and 2.07 reported earlier and also indicates that bore hoop stress is increased, as a result of the presence of the holes, by around 7% above the Lamé value for a plain tube, also shown in Figure 5.

The above results may be compared (for the case of the offset ellipse) with those obtained independently using the ABAQUS program which gave the results illustrated by filled squares in Figure 5. Agreement is within 2%.

## Commentary

1. The elastic FE results conform with the elastic predictions based on existing SCF data are reasonable.
2. The critical location based on elastic stress concentration at the hole is the point on the hole nearest the bore, although at certain ellipse eccentricities the SCF at the point on the channel radially opposite the critical point exhibits stresses which are only 25% lower than the critical location.
3. The presence of the holes raises bore stresses above the Lamé predictions by around 7%.

## ELASTIC-PLASTIC FINITE ELEMENT ANALYSIS

In the final phase of the numerical analysis a full elastic-plastic Finite Element analysis was undertaken using the NISA FE package to perform a limited number of Elastic/Plastic calculations to assess the level of the residual stresses which are 'locked' into the tube in the vicinity of the hole and elsewhere. Full details of the procedure are given in [9].

In this analysis a radial bore displacement equivalent to that required to achieve a given nominal percentage overstrain in a plain tube (i.e. one without axial holes) was applied to the bore of the cylinder and plastic flow permitted (based upon Tresca's yield criterion). A plot of the contours of plastic strain at the peak of a typical loading (for 60% autofrettage) is shown in Figure 6; these results are discussed later. The displacement condition was subsequently removed and the bore permitted to relax to a stress free state. This unloading is elastic in all the cases considered (i.e. there is no reversed yielding).

The most interesting features of the residual stresses are shown in Figure 7 and Figure 8. The residual hoop stresses on a radial line from bore to hole boundary are particularly interesting. Figure 7 relates to equal 60% nominal overstrains applied to Case 1 and Case 2 geometries in which the stress at the peak of the autofrettage process is capped at yield magnitude (tensile) at the hole boundary. Subsequent removal of the bore loading produces elastic unloading with the stress concentration effect of the hole dominating the resulting residual stress field near the hole boundary. The hole with the higher SCF produces the higher magnitude of compressive residual stress since the SCF is effective during the entire elastic unloading process. However, at points removed from the hole boundary, and particularly near the bore, the residual stress patterns are effectively coincident.

If a working (normally cyclic) pressure is now applied to the bore there is an elastic re-loading to a level below that which was achieved at the peak of the autofrettage process. Since the compressive residual stress at the hole is of greater magnitude in the case of the higher SCF, the maximum stress (and hence stress range) at the hole boundary is highest for the semi-ellipse (a somewhat surprising result). However there is a peak in the stress range some distance from the hole which is effectively coincident for both hole shapes. For the semi-ellipse the stress

range at this point is some 12% higher than that at the hole boundary whilst it is 22% higher for the semi-circle. The implication of this is that failure may initiate within the material a small distance from the hole boundary. However experience indicates that the more likely failure initiation locations are at the hole surface because manufacturing processes are far more likely to cause defects at a surface.

Figure 8 relates to a fixed geometry (Case 1 - the semi-circular hole) and compares four examples of autofrettage arising from radial bore displacements equivalent to 20%, 40%, 60% and 80% nominal overstrain in plain tubes.

The elastic/plastic analysis gives a residual stress at the bore which is significantly lower than that for a plain tube [10]. The comparison is shown in Table 2. Thus, levels of bore residual stress in the perforated tube are, for overstrains exceeding 40%, generally some 15% lower than the equivalent figure in the plain tube.

Figure 6, showing plastic strain contours for 60% nominal overstrain, provides additional convincing evidence for the effect of the holes upon the overstrain process. A 45 degree 'slip line' emanating from the corner of the hole is clearly visible, implying that a significant part of bore displacement effect will simply be lost as a result of this slip mechanism. By a simple iterative calculation we find that the value of 50% of yield predicted by the Finite Element analysis for 60% overstrain of a perforated tube would be caused by 44% overstrain of a plain tube.

## Commentary

1. The Finite Element predictions of compressive residual hoop stresses at the hole are of greatest magnitude in the case of the higher SCF.
2. For a fixed value of nominal overstrain and different hole geometries the residual stress patterns at points removed from the hole are almost coincident, with virtually identical values at the bore.
3. The peak value of residual stress is slightly positive and occurs some 2.5mm from the hole. This is also the region of maximum applied plus residual hoop stress when the tube is repressurized to a working pressure below that required for autofrettage. Thus the stress range is maximum which implies that failures may initiate a small distance from the hole boundary. However experience indicates that the more likely failure initiation locations are at the hole surface.
4. For the hole size and location investigated the residual hoop stress at the bore is reduced by approximately 15% below the value for a plain tube of the same radius ratio for nominal overstrains of 40% or greater. This effect is ascribed to the reduction of constraint arising from the presence of the holes which results in a slip-line pattern dominated by the holes.

## X-RAY MEASUREMENTS OF RESIDUAL STRESS

An experimental investigation using X-ray diffraction methods, applied to specimens of similar material and geometry subjected to 60% nominal overstrain, was undertaken. The results for the particular area of interest here, namely the residual hoop stresses on the radial line from bore to a semi-circular hole and beyond, are presented as discrete data points in Figure 9.

The results presented in Figure 9 were obtained for a specimen having the same hole geometry as in Figure 2 but with a reduced bore radius (79.5mm) and a reduced outer radius (143.5mm), hence the ratio is 1.805. Figure 9 shows the measured residual stresses; these results were modified, by a simple vertical shifting, to ensure that equilibrium is satisfied by achieving equal areas above and below the horizontal axis. This leads to the conclusion that the compressive residual stress at the bore is 50% of yield. As noted previously a plain tube of this radius ratio requires 44% overstrain to achieve such a figure, and an ideal elastic/plastic plot for a plain cylinder of the same radius ratio subjected to 44% autofrettage is shown as a continuous line in Figure 9. Agreement in the important region of potential crack growth near the bore is good; the 44% line provides a slightly conservative bound and is recommended for design purposes. (Note: the bound is conservative since the stresses are compressive and the bound represents a lower proportion of these stresses near the bore).

Agreement between experimental and Finite Element residual stress predictions is generally considered acceptable. The most significant discrepancy between the experimental results of Figure 9 and FE results of Figure 8 is in the immediate vicinity of the hole. Whilst a positive peak is evident from the experimental results, the sharp reduction to relatively large compressive residual stress is absent. This lack of compressive residual stress is believed to be real and somewhat unsurprising. In the case of autofrettage of a plain tube the high compressive residual stress at the bore predicted by the ideal elastic-plastic analysis is not achieved. This reduction is frequently associated with the Bauschinger effect [11] in which the yield strength in compression is significantly reduced as a result of prior yielding in tension. However, in the case of yielding in the vicinity of the hole this effect may be compounded by an extremely high stress gradient. No attempt is made at this stage to quantify or separate these two effects.

## RING SLICING ANALYSIS OF RESIDUAL STRESS

In the safe fatigue life testing of autofrettaged tubes it is now common practice to cut relatively thin (25mm or thereabouts) ring samples and to slice these rings radially in order to measure the angle of opening. This angle of opening is a direct measure of the bending moment 'locked in' to the tube during autofrettage, and subsequently released as the tube is sliced. It is possible to calculate the opening for any given percentage overstrain of a plain tube based upon an 'ideal' elastic/perfectly plastic analysis, see appendix to [12]. Any reduction in opening below the anticipated amount is an indication that the desired 'ideal' autofrettage residual stresses have not been achieved.

If material is removed from inner and/or outer radii such that the remaining (thinner) tube is composed entirely of material which has experienced plastic strain a straightforward superposition of the 'ideal' autofrettage residual stress fields indicates that this thinner tube contains precisely those residual stresses which would have been locked in by 100% overstrain of its final dimensions. Hence it is possible to predict the opening of such a thinner tube when sliced.

A ring specimen of inner radius 82.5 mm and outer radius 152.5mm was cut from a perforated tube containing semi-circular holes and the material beyond the holes was subsequently removed. Hence the remaining specimen resembled the geometry illustrated in Figure 10. Because of the loss of constraint resulting from the (now) multiple, external, semi-circular notches the specimen is assumed to have inner radius 82.5 mm and outer radius 108 mm (the radial distance to the nearest point on the hole). When cut, this tube opened by only 69.5% of the 'ideal' figure for 100% overstrain of such a tube calculated from the equations in [12].

Referring back to the experimental residual stress results of Figure 9 it is possible to confine attention to the radii range from 82.5 mm to 108 mm. By superposition the net force over this range was put to zero and the locked-in bending moment was calculated numerically. This moment equated to 71% of the moment arising from 'ideal' 100% overstrain. This gives further support to the validity of the experimentally determined residual stress measurements. Furthermore, because of the extreme sensitivity of the bending moment calculation to changes in stress near the inner radius and the hole boundary of the thinner tube, this is taken as support for the assumption that the residual stresses near the hole do not exhibit the large downturn predicted by the FE analyses.

## Recommendations

In order to achieve conservative design it is recommended that:

- a. Zero residual hoop stresses be assumed at the hole; this will also ensure that the full stress range is identified in the event of slightly tensile stresses.
- b. Bore residual hoop stresses equivalent to those determined by the Finite Element analysis be assumed to exist in the perforated tube.
- c. Elastic cyclic loading higher than that for a plain tube must be used at the bore and hole; this requires bore hoop stress some 7% above that for a plain tube, and hole hoop stress some 264% above that for a plain tube at the equivalent location.

## IMPLICATIONS FOR FATIGUE LIFETIME

Data relating to fatigue lifetimes at the bore of plain and perforated tubes are presented in Table 3.

Referring to Equation 4 and recognising that the stress range at the bore in a plain, tested specimen is analogous to  $\Delta\sigma_1$  it is possible to calculate the stress range at the bore in the new design which contains axial holes, by recognising that this is equivalent to  $\Delta\sigma_2$ . For this calculation we assume that the initial cracking that could be caused by heat checking, is identical in both cases. Hence we can calculate, via equation 5, a predicted lifetime for the perforated design using the elastic-plastic FE results discussed previously. These predictions are shown in the right hand column of Table 3. Information is provided for two values of yield strength.

Turning now to the lifetime at the hole we can use Equation 5 again, but this time we assume zero residual stress at the hole, a stress range due to the SCF of 2.61 calculated previously and use the equation to calculate the ratio of the initial defect sizes. A ratio of 58.8:1 (bore:hole) is obtained, which confirms the relatively large initial defect size at the bore resulting from 'heat-checking' during initial firing. These data are presented in Table 4. It is also possible to calculate lifetime for the semi-elliptical hole with its SCF of 2.07. An improvement in lifetime by a factor of two is predicted as a result of the semi-elliptical design.

#### Commentary

1. The design methodology provides good predictions of lifetimes for failure from the bore for a range of autofrettaged tubes with varying internal cutouts, radius ratios and percentage overstrains which had similar pre-existing defects.

2. These predictions are all in excess of the experimentally determined lifetimes for cracks emanating from the hole based upon an initial crack length at the bore some 58.8 times that at the hole. For the semi-circular design the average ratio of lifetime at the bore to lifetime at the hole is approximately 1.6.

3. Assuming that the residual stress at the hole boundary is zero or slightly positive there is approximately a factor of 2 increase in lifetime as a result of changing from a semi-circular to a semi-elliptical hole.

#### **SUMMARY AND CONCLUSIONS**

This work addressed the fatigue lifetimes of thick cylinders containing multiple, axial holes within the wall. The holes are generally semi-elliptical (including semi-circular) and the cylinders are autofrettaged after introduction of the holes and are subsequently subjected to cyclic pressurization of the bore.

A model for the prediction of lifetime based upon pre-existing crack-like defects at two potentially critical locations was developed. A comprehensive study, incorporating elastic and elastic-plastic Finite Element analyses, residual stress measurement by X-ray diffraction and tube opening tests on overstrained cylinders, has been described. Finally, fatigue lifetime comparisons and predictions were undertaken on the basis of these numerical and experimental results and of existing fatigue lifetime data. These various elements, when assembled, indicate:

1. The critical location based on elastic stress concentration at the hole is the point on the hole nearest the bore, although at certain ellipse eccentricities the SCF at the point on the hole radially opposite the critical point exhibits stresses which are only 25% lower than the critical location.

2. The presence of coolant channels raises bore stresses above the Lamé predictions by about 7%.

3. The Finite Element results predict significant compressive residual hoop stresses at the hole with greater magnitude in the case of the higher SCF. However, the X-ray measurements of residual stress show zero or slightly tensile residual stresses at the hole. In this region Bauschinger and high stress gradient effects may operate separately or together to reduce the compressive stresses.

4. For a fixed value of nominal overstrain and different hole geometries the residual stress patterns at points removed from the hole are almost coincident, with virtually identical values at the bore.

5. The peak value of residual stress is slightly positive and occurs some 2.5mm from the hole. This is also the region of maximum hoop stress (and hence tensile stress range) when the tube is repressurized to a working pressure below that required for autofrettage; this implies that failures may initiate a small distance from the hole boundary. However experience indicates that the more likely failure initiation locations are at the hole surface.

6. For a given hole size and location and for nominal overstrains of 40% or greater the residual compressive stress at the bore is reduced by approximately 15% below the value for a plain tube of the same radius ratio. This supports the hypothesis that it is loss of constraint from material beyond the holes which produces this effect. These results were compared with experimental (X-ray diffraction) data and other data from tube slicing tests, both of which reinforce the conclusion.

These findings and recommendations lead to a predicted lifetime for a tube with axial holes and indicate that the critical location for fatigue failure is the hole boundary. For semi-circular holes the ratio of lifetime at bore to that at hole is approximately 1.6.

#### **ACKNOWLEDGEMENTS**

Three of the authors (APP, SNE and TJB) acknowledge partial support for this work via the European Research Office of the US Army Research, Development and Standardization Group (UK).

## REFERENCES

STP 791, American Society for Testing and Materials, pp  
I216-I237

1. Underwood, J. H., and Parker, A. P., 1995, "Fatigue Life Analysis and Tests for Thick-Wall Cylinders Including Effects of Overstrain and Axial Grooves", *ASME Journal of Pressure Vessel Technology*, Vol 117, pp222-226
2. Parker, A. P., and Underwood, J. H., 1995, "Stress Concentration, Stress Intensity and Fatigue Crack Growth Along Evacuators of Pressurized, Autofrettagged Tubes", ASME PVP Conference Proceedings, Hawaii, 1995 (In Press ASME PVT Journal, 1996)
3. Endersby, S. N., Bond, T. J. and Parker A. P., 1996, "Stress Concentration, Stress Intensity and Fatigue Crack Growth Along Angled Evacuators of Pressurized, Autofrettagged Tubes" (In preparation for publication)
4. Parker, A. P., and Underwood, J. H., 1997, "Some Methods of Representing Fatigue Lifetime as a Function of Stress Range and Initial Crack Length", presented at 28th National Symposium on Fatigue and Fracture Mechanics, Saratoga Springs, June 1996, to be published in *Fatigue and Fracture Mechanics: 28th Volume, ASTM STP 1321*, J. H. Underwood, B. D. MacDonald and M. R. Mitchell, Eds, American Society for Testing and Materials
5. Parker, A. P., and Underwood, J. H., "A Rapid Method for Determining Stress Concentrations for Autofrettagged Tubes Containing Multiple Axial Perforations Within the Wall" *Technical Report, Watervliet Arsenal, Watervliet, NY*, 1996 ARCCB-CR-96025
6. Peterson, R. E., 1974, *Stress Concentration Factors*, Wiley, New York
7. Nisitani, H., 1968, "Method of Approximate Calculation for Interference of Notch Effect and its Application", *Bull Japan Soc Mech Eng*, 11, p725
8. Schulz, K. J., "On the State of Stress in Perforated Strips and Plates", *Proc Koninklyke Nederlandsche Akadamie van Wetenschappen (Netherlands Royal Academy of Science)*, Amsterdam, (6 papers) Vol 45, pp233, 341, 457, 524 (1942) Vol 46-48, pp 282, 292 (1943-45)
9. Endersby, S.N., PhD Thesis, University of Northumbria at Newcastle, Newcastle, England (Submission September 1997)
10. Hill, R., 1950, *The Mathematical Theory of Plasticity*, Clarendon Press, Oxford
11. Milligan, R. V., Koo, W. H., and Davidson, T. E., "The Bauschinger Effect in a High-Strength Steel", *Journal of Basic Engineering*, Vol 88, 1966, pp 480-488
12. Parker, A. P., Underwood, J. H., Throop, J. F. and Andrasic, C. P., 1983, "Stress Intensity and Fatigue Crack Growth in a Pressurized, Autofrettagged Thick Cylinder", *ASTM*

CASE	b/a	offset(a'/a)	LOCATION OF Kt	
			A	B
1 (semi-circle)	1	0	2.64	1.53
2 (offset ellipse)	2	0.5	2.07	1.51
3 (semi-ellipse)	0.5	0	4.06	1.82
4 (semi-ellipse)	2	0	2.04	1.48
5 (semi-ellipse)	1.5	0	2.25	1.46
6 (semi-ellipse)	2.5	0	1.91	1.4
7 (semi-ellipse)	0.75	0	3.2	1.69

**Table 1: Effect of Hole Eccentricity on Stress Concentration Factor**

Percentage Autofrettage	Percentage of Yield at Bore (Plain Tube)	Percentage of Yield at Bore (FE Analysis)
20	27.5	25
40	47.2	39
60	60.3	50
80	67.6	59

**Table 2 : Reduced Bore Compressive Hoop Stress**

	R2	R1	Yield	overstrain	Firing Press	Stress range(ID)	Life(Plain Tube)	Predicted (Perforated Design)
	(mm)	(mm)	(MPa)	(%)	(MPa)	(MPa)	(cycles)	(cycles)
Plain	142.2	89	1,240	60	393	717.8	10,873	
Perforated	152.4	84.5	1,240	*44	406	605.6		18,150
Perforated	152.4	84.5	1,104	*44	406	673.6		13,189

\*indicates overstrain for equivalent plain tube

**TABLE 3 : Lifetimes for pre-cracked Tubes with Semi-circular Holes, Failure Originating from Bore**

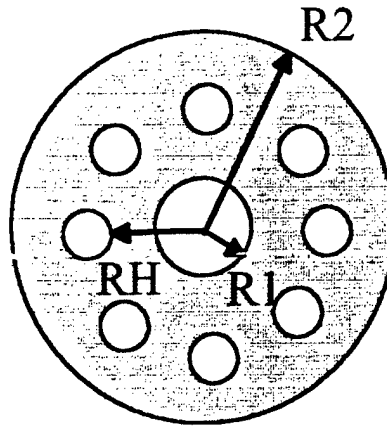
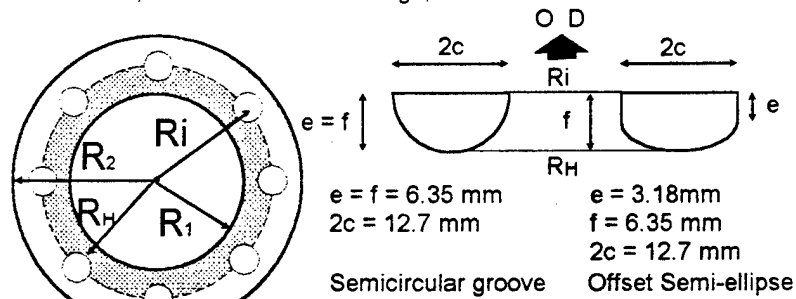


**Figure 1: Schematic Illustration of Geometry Considered**  
 (Note, Axial holes may be of various cross-sectional shapes)

**Axial Perforations - Geometry & Loading**

24 Grooves, 60% & 80% Autofrettage, Yield 1100 MPa & 1240 MPa



$R_1 = 84.5 \text{ mm}$

$R_i = 114 \text{ mm}$

$R_2 = 152.5 \text{ mm}$

Note : zero interference

TEST & FIRING PRESSURE :  
 406 MPa

**Figure 2: Specific Hole Geometries Analysed Using Finite Element Methods**

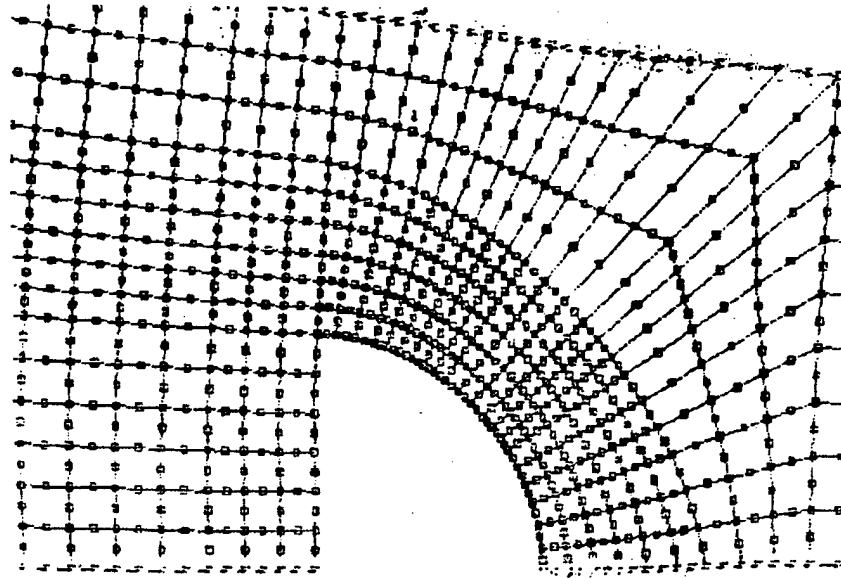


Figure 3 : Typical Finite Element Mesh Used in Stress Analysis

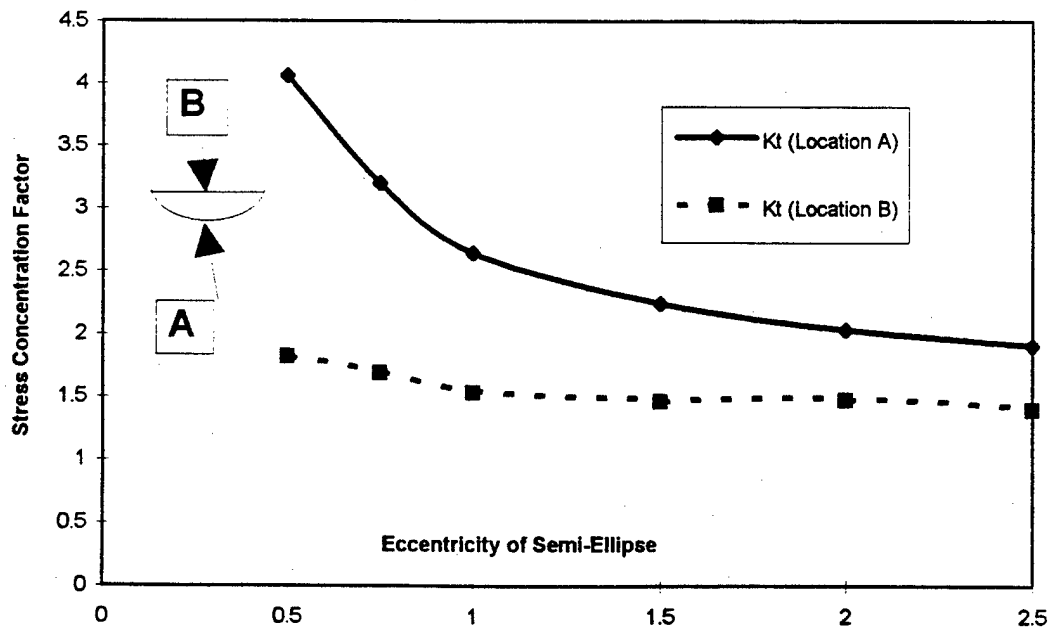


Figure 4 : Relationship Between Eccentricity of Semi-Ellipse (b/a) and Stress Concentration Factor (Kt)

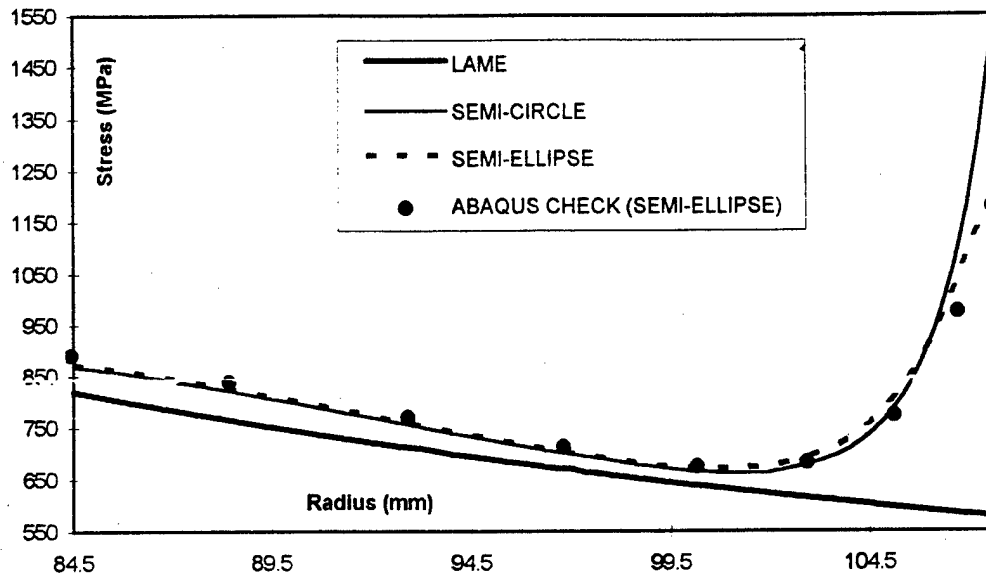


Figure 5 : Hoop Stresses in Perforated Tube,  
Bore to Hole - Bore Pressure 434 MPa

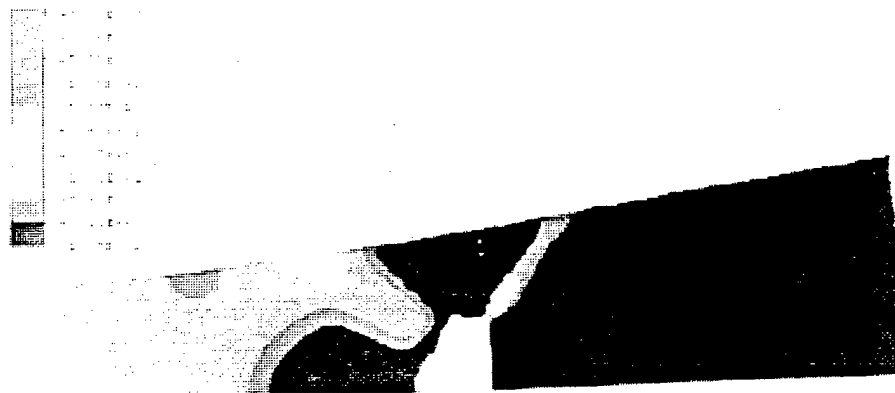


Figure 6 : Contours of Plastic Strain at Peak of Autofrettage Cycle

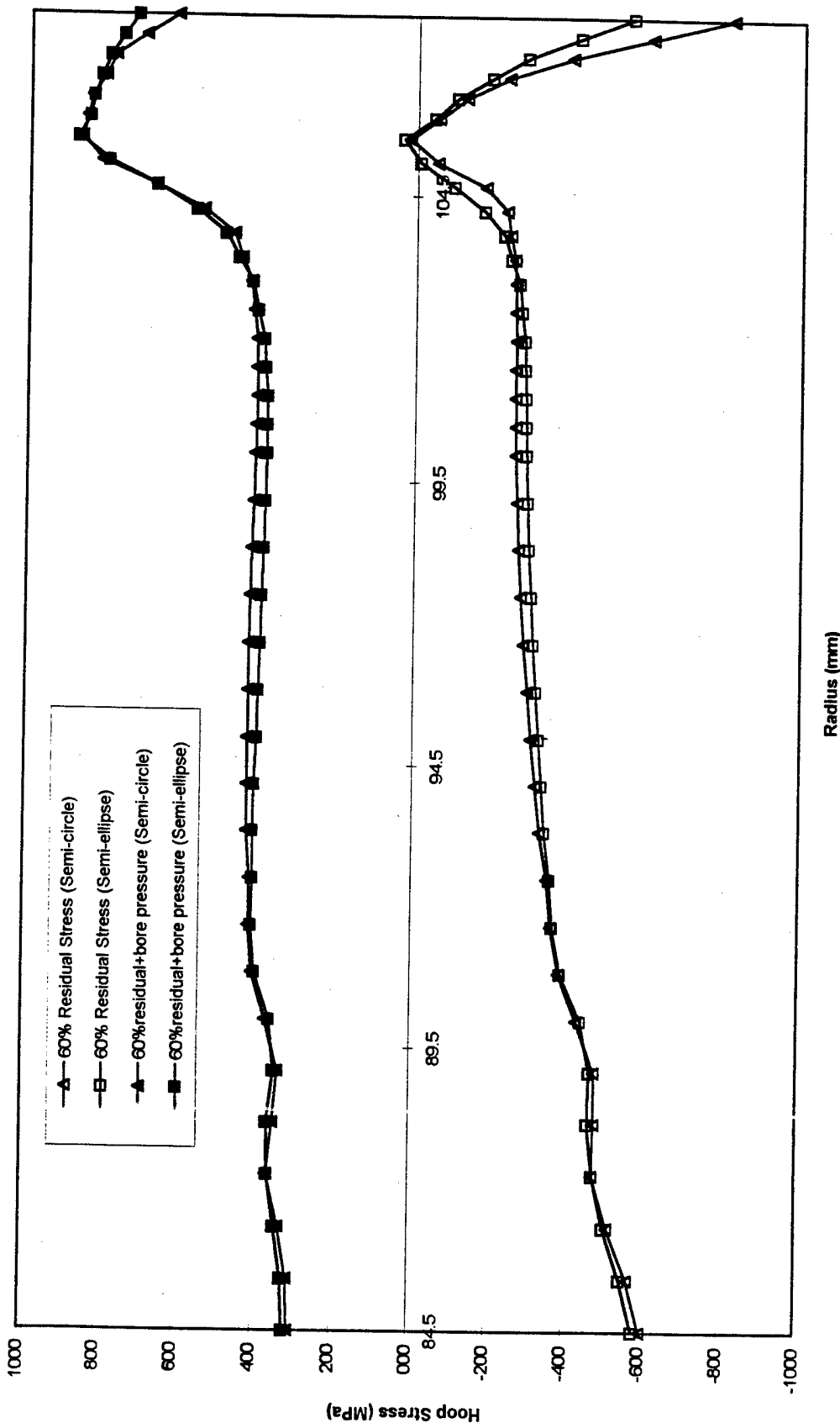


Figure 7 : 60% Nominal Swage Autofrettage Stresses  
Semi-circular and Offset Semi-elliptical Holes

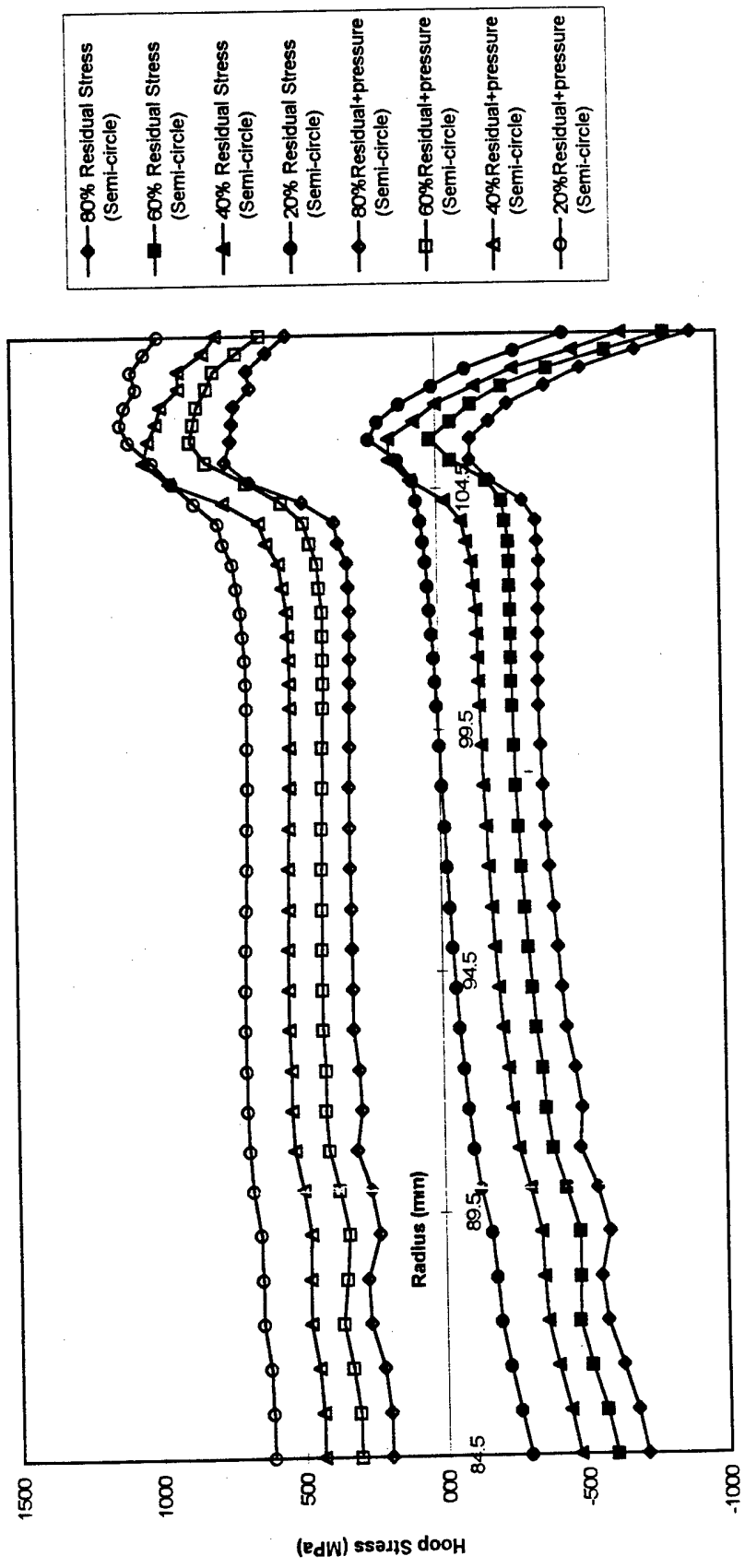


Figure 8 : Swage Autofrettage with Semi-Circular Holes -  
20%, 40%, 60%, 80% Nominal Overstrain

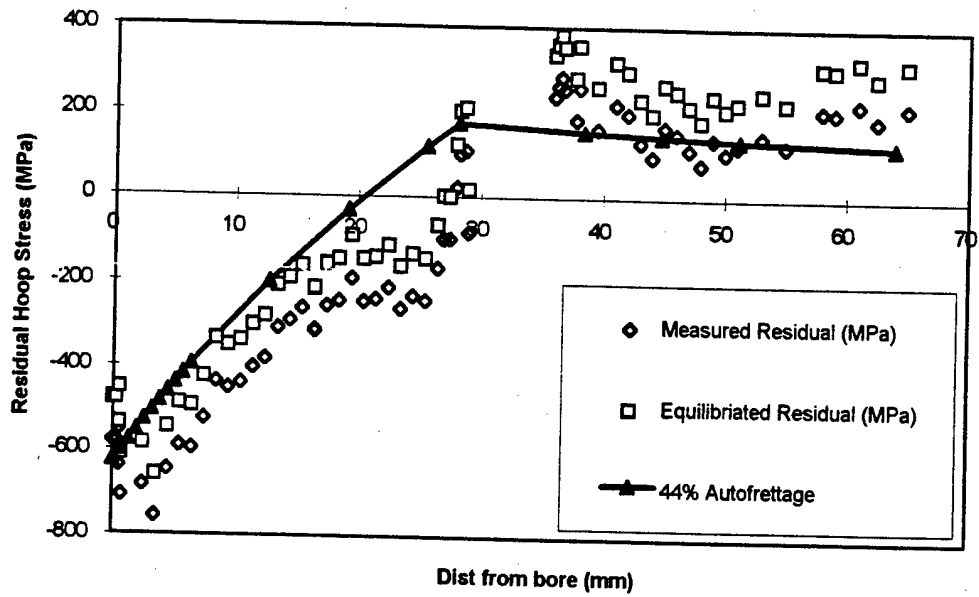


Figure 9 : X-Ray Diffraction Residual Stress Measurements Compared to Proposed Bound

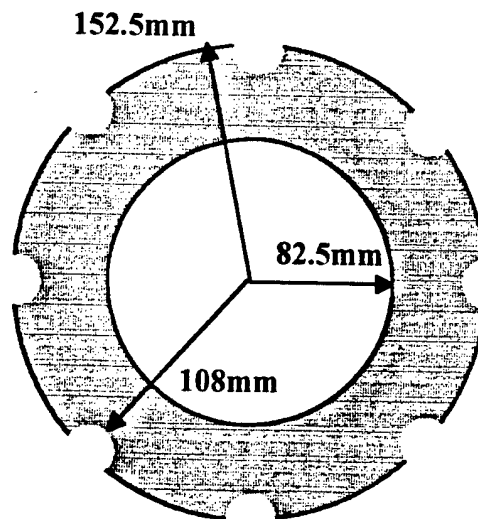


Figure 10 : Form of Remaining, Inner Externally Notched Tube which was Subsequently Opened by Radial Slitting

---

TECHNICAL REPORT INTERNAL DISTRIBUTION LIST

	<u>NO. OF COPIES</u>
CHIEF, DEVELOPMENT ENGINEERING DIVISION	
ATTN: AMSTA-AR-CCB-DA	1
-DB	1
-DC	1
-DD	1
-DE	1
CHIEF, ENGINEERING DIVISION	
ATTN: AMSTA-AR-CCB-E	1
-EA	1
-EB	1
-EC	1
CHIEF, TECHNOLOGY DIVISION	
ATTN: AMSTA-AR-CCB-T	2
-TA	1
-TB	1
-TC	1
TECHNICAL LIBRARY	
ATTN: AMSTA-AR-CCB-O	5
TECHNICAL PUBLICATIONS & EDITING SECTION	
ATTN: AMSTA-AR-CCB-O	3
OPERATIONS DIRECTORATE	
ATTN: SIOWV-ODP-P	1
DIRECTOR, PROCUREMENT & CONTRACTING DIRECTORATE	
ATTN: SIOWV-PP	1
DIRECTOR, PRODUCT ASSURANCE & TEST DIRECTORATE	
ATTN: SIOWV-QA	1

NOTE: PLEASE NOTIFY DIRECTOR, BENÉT LABORATORIES, ATTN: AMSTA-AR-CCB-O OF ADDRESS CHANGES.

---

---

TECHNICAL REPORT EXTERNAL DISTRIBUTION LIST

	<u>NO. OF COPIES</u>		<u>NO. OF COPIES</u>
ASST SEC OF THE ARMY RESEARCH AND DEVELOPMENT ATTN: DEPT FOR SCI AND TECH THE PENTAGON WASHINGTON, D.C. 20310-0103	1	COMMANDER ROCK ISLAND ARSENAL ATTN: SMCRI-SEM ROCK ISLAND, IL 61299-5001	1
DEFENSE TECHNICAL INFO CENTER ATTN: DTIC-OCP (ACQUISITIONS) 8725 JOHN J. KINGMAN ROAD STE 0944 FT. BELVOIR, VA 22060-6218	2	MIAC/CINDAS PURDUE UNIVERSITY 2595 YEAGER ROAD WEST LAFAYETTE, IN 47906-1398	1
COMMANDER U.S. ARMY ARDEC ATTN: AMSTA-AR-AEE, BLDG. 3022	1	COMMANDER U.S. ARMY TANK-AUTMV R&D COMMAND ATTN: AMSTA-DDL (TECH LIBRARY) WARREN, MI 48397-5000	1
AMSTA-AR-AES, BLDG. 321	1	COMMANDER	
AMSTA-AR-AET-O, BLDG. 183	1	U.S. MILITARY ACADEMY	
AMSTA-AR-FSA, BLDG. 354	1	ATTN: DEPARTMENT OF MECHANICS	1
AMSTA-AR-FSM-E	1	WEST POINT, NY 10966-1792	
AMSTA-AR-FSS-D, BLDG. 94	1		
AMSTA-AR-IMC, BLDG. 59	2	U.S. ARMY MISSILE COMMAND	
PICATINNY ARSENAL, NJ 07806-5000		REDSTONE SCIENTIFIC INFO CENTER	2
		ATTN: AMSMI-RD-CS-R/DOCUMENTS BLDG. 4484	
DIRECTOR U.S. ARMY RESEARCH LABORATORY ATTN: AMSRL-DD-T, BLDG. 305	1	REDSTONE ARSENAL, AL 35898-5241	
ABERDEEN PROVING GROUND, MD 21005-5066		COMMANDER	
		U.S. ARMY FOREIGN SCI & TECH CENTER	
DIRECTOR U.S. ARMY RESEARCH LABORATORY ATTN: AMSRL-WT-PD (DR. B. BURNS)	1	ATTN: DRXST-SD	1
ABERDEEN PROVING GROUND, MD 21005-5066		220 7TH STREET, N.E.	
		CHARLOTTESVILLE, VA 22901	
DIRECTOR U.S. MATERIEL SYSTEMS ANALYSIS ACTV ATTN: AMXSY-MP	1	COMMANDER	
ABERDEEN PROVING GROUND, MD 21005-5071		U.S. ARMY LABCOM, ISA	
		ATTN: SLCIS-IM-TL	1
		2800 POWER MILL ROAD	
		ADELPHI, MD 20783-1145	

---

NOTE: PLEASE NOTIFY COMMANDER, ARMAMENT RESEARCH, DEVELOPMENT, AND ENGINEERING CENTER,  
BENÉT LABORATORIES, CCAC, U.S. ARMY TANK-AUTOMOTIVE AND ARMAMENTS COMMAND,  
AMSTA-AR-CCB-O, WATERVLIET, NY 12189-4050 OF ADDRESS CHANGES.

---

TECHNICAL REPORT EXTERNAL DISTRIBUTION LIST (CONT'D)

	<u>NO. OF COPIES</u>		<u>NO. OF COPIES</u>
COMMANDER U.S. ARMY RESEARCH OFFICE ATTN: CHIEF, IPO P.O. BOX 12211 RESEARCH TRIANGLE PARK, NC 27709-2211	1	WRIGHT LABORATORY ARMAMENT DIRECTORATE ATTN: WL/MNM EGLIN AFB, FL 32542-6810	1
DIRECTOR U.S. NAVAL RESEARCH LABORATORY ATTN: MATERIALS SCI & TECH DIV WASHINGTON, D.C. 20375	1	WRIGHT LABORATORY ARMAMENT DIRECTORATE ATTN: WL/MNMF EGLIN AFB, FL 32542-6810	1

NOTE: PLEASE NOTIFY COMMANDER, ARMAMENT RESEARCH, DEVELOPMENT, AND ENGINEERING CENTER,  
 BENÉT LABORATORIES, CCAC, U.S. ARMY TANK-AUTOMOTIVE AND ARMAMENTS COMMAND,  
 AMSTA-AR-CCB-O, WATERVLIET, NY 12189-4050 OF ADDRESS CHANGES.

---